

# Late Ediacaran organic microfossils from Finland

Sebastian Willman  and Ben J. Slater 

Department of Earth Sciences, Palaeobiology, Uppsala University, Villavägen 16, SE-75236, Uppsala, Sweden

## Original Article

**Cite this article:** Willman S and Slater BJ (2021) Late Ediacaran organic microfossils from Finland. *Geological Magazine* **158**: 2231–2244. <https://doi.org/10.1017/S0016756821000753>

Received: 16 March 2021  
Revised: 10 June 2021  
Accepted: 24 June 2021  
First published online: 24 August 2021

### Keywords:

Ediacaran; Bilateria; microbial mats; acritarchs; impact crater; organic-walled microfossils; Baltica

### Author for correspondence:

Sebastian Willman,  
Email: [Sebastian.Willman@geo.uu.se](mailto:Sebastian.Willman@geo.uu.se);  
Ben Slater,  
Email: [Ben.Slater@geo.uu.se](mailto:Ben.Slater@geo.uu.se)

## Abstract

Here we present a detailed accounting of organic microfossils from late Ediacaran sediments of Finland, from the island of Hailuoto (northwest Finnish coast), and the Saarijärvi meteorite impact structure (~170 km northeast of Hailuoto, mainland Finland). Fossils were recovered from fine-grained thermally immature mudstones and siltstones and are preserved in exquisite detail. The majority of recovered forms are sourced from filamentous prokaryotic and protistan-grade organisms forming interwoven microbial mats. Flattened *Nostoc*-ball-like masses of bundled *Siphonophycus* filaments are abundant, alongside *Rugosoopsis* and *Palaeolyngbya* of probable cyanobacterial origin. Acritarchs include *Chuarina*, *Leiosphaeridia*, *Symphlassosphaeridium* and *Synsphaeridium*. Significantly, rare spine-shaped sclerites of bilaterian origin were recovered, providing new evidence for a nascent bilaterian fauna in the terminal Ediacaran. These findings offer a direct body-fossil insight into Ediacaran mat-forming microbial communities, and demonstrate that alongside trace fossils, detection of a bilaterian fauna prior to the Cambrian might also be sought among the emerging record of small carbonaceous fossils (SCFs).

## 1. Introduction

The latest part of the Ediacaran System harbours signatures for some of the most important changes in the history of the biosphere. Multiple lines of fossil evidence indicate that many of the foundations of animal-dominated Phanerozoic-style ecosystems were assembled at this time, and include structurally complex Ediacaran macrofossils (e.g. Liu *et al.* 2014; Ivantsov *et al.* 2019a), animal-derived biomarkers (Bobrovskiy *et al.* 2018a), possible metazoan reefs (Grotzinger *et al.* 2005; Penny *et al.* 2014) and the advent of macroscopic biomineralization (e.g. *Cloudina* (Grant, 1990)). Perhaps most significantly, a trace fossil record of complex horizontal burrows and trails appears from ~560 Ma, likely documenting the emergence of a bilaterian benthos (Martin *et al.* 2000; Jensen, 2003; Chen *et al.* 2013, 2019; Budd, 2015; Budd & Jensen, 2017). These simple trace fossils are consistently found in association with bedding planes exhibiting microbial mat textures, and have been interpreted as representing a variety of mat-exploiting behaviours (Buatois *et al.* 2014; Meyer *et al.* 2014; Tarhan *et al.* 2017; Ivantsov *et al.* 2019b). Together, these lines of evidence point to a characteristic Ediacaran matground ecology which appears to have persisted into the early Cambrian Fortunian (Buatois *et al.* 2014; Laing *et al.* 2019). Despite the importance of these environments as cradles of early animal evolution (Budd & Jensen, 2017), there is currently little direct accounting of body fossils either from the biomat-forming organisms, or from the nascent bilaterian fauna themselves.

Organic walled microfossils (OWMs) are one source of direct body-fossil data that can be retrieved from siliciclastic rocks. Most studies of OWMs from the Ediacaran to date have focused on acritarchs (e.g. Moczyłowska, 2005; Willman *et al.* 2006). In studies of comparable OWM-bearing deposits from the Cambrian, there has recently been an increased awareness that a larger size class of organically preserved remains is accessible if a gentler processing procedure is applied. These larger, more delicate forms have been dubbed small carbonaceous fossils (SCFs), and encompass a polyphyletic mix of organic remains sourced from various organisms, including the fragmentary remains of metazoans (Butterfield & Harvey, 2012). Recently, several SCF biotas have been recovered from early Cambrian sediments in the Baltic region (Slater *et al.* 2017; Guilbaud *et al.* 2018; Kesidis *et al.* 2019; Slater & Willman, 2019), including from earliest Cambrian strata (Slater *et al.* 2018a). Extending this record into the Ediacaran is crucial for capturing SCF diversity contemporaneous with the earliest stages of bilaterian evolution.

Finland is one region of Baltica that has been relatively under-explored in terms of its Ediacaran fossil record. Nevertheless, several localities preserving sediments of Ediacaran age are found in Finland, and crucially the thermal immaturity of these sediments makes them ideally suited for SCF preservation (Slater & Willman, 2019). Here we report a rich record of organic microfossils from a late Ediacaran sequence in Finland, from Hailuoto Island and the Saarijärvi meteorite impact crater (Fig. 1).

© The Author(s), 2021. Published by Cambridge University Press. This is an Open Access article, distributed under the terms of the Creative Commons Attribution licence (<http://creativecommons.org/licenses/by/4.0/>), which permits unrestricted re-use, distribution and reproduction, provided the original article is properly cited.

**CAMBRIDGE**  
UNIVERSITY PRESS

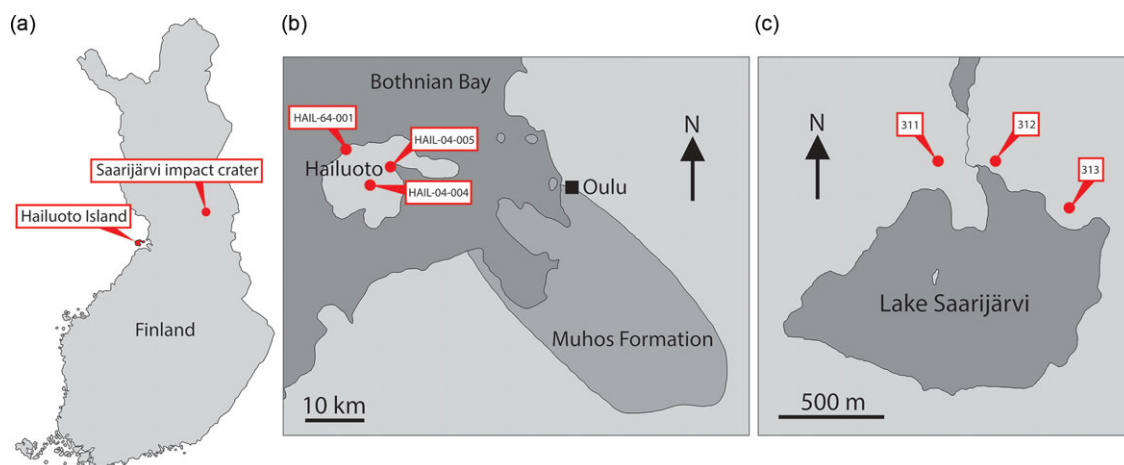


**Fig. 1.** (Colour online) (a) Map of Finland showing location of Hailuoto Island and the Saarijärvi impact structure. (b) Map showing Hailuoto Island in relation to the onshore Muhos basin, and core localities. (c) Map showing Lake Saarijärvi within the Saarijärvi impact structure and position of core localities. (Based on Klein *et al.* 2015, fig. 1; Solismaa, 2008, fig. 4; Öhman & Preeden, 2013, fig. 3.)

## 2. Geological setting

An extended episode of erosion during the early- to mid-Neoproterozoic era left Baltica as a peneplained continent of exceptionally low relief (Lidmar-Bergström, 1993, 1995). Subsequent transgressions during the late Neoproterozoic and early Phanerozoic flooded large regions of this topographically flat landscape, resulting in extensive shallow marine deposition (Nielsen & Schovsbo, 2011). Siliciclastic sediments deposited in these epeiric seaways extend over large regions of the Bothnian Sea and the Baltic states. Based on the thickening trend of these sediments toward the Finnish coastline, equivalent deposits are thought to have once covered much of Finland (Puura *et al.* 1996; Kohonen & Rämö, 2005; Bogdanova *et al.* 2008; Klein *et al.* 2015; Slater & Willman, 2019). In Finland, even more than elsewhere in Baltica, the vast majority of these sediments have subsequently been eroded and now remain only as relatively small and geographically scattered outliers.

One region where a substantial portion of late Neoproterozoic sediments has survived in Finland is the island of Hailuoto (Fig. 1). Hailuoto is situated in the Bothnian Bay off the northwest coast of the Finnish mainland, west of the coastal city of Oulu (Fig. 1). Beneath a covering of Quaternary sediments lies the subsurface Hailuoto Formation (known entirely from drillcore), a package of sandstones, mudstones, siltstones, clays and conglomerates which varies in thickness across the island, reaching a maximum thickness of ~560 m (Solismaa, 2008; Klein *et al.* 2015). The upper ~55–65 m of the formation consists of greenish-grey fine-grained sandstones, shales and siltstones. Below this are deposited red-coloured arkosic sandstones and shales, which rest unconformably on the crystalline basement or on sediments of the Mesoproterozoic–Neoproterozoic Muhos Formation which underlies much of the Bothnian Bay and outcrops adjacent to Hailuoto on the Finnish mainland (Fig. 1). The Muhos Formation consists of red-green-grey siltstones and shales (Kohonen & Rämö, 2005), similar in lithology to the Hailuoto Formation (Tynni & Siivola, 1966; Tynni & Donner, 1980; Kohonen & Rämö, 2005; Solismaa, 2008; Klein *et al.* 2015).

Based on correlation with adjacent strata and its microfossil contents, the Hailuoto Formation is considered to be late Neoproterozoic in age, with estimates in the range of 600–570 Ma (Veltheim, 1969; Tynni & Donner, 1980; Paulamäki & Kuivamäki,

2006; Klein *et al.* 2015; Luukas *et al.* 2017). This would place the deposition of the Hailuoto Formation in approximately the middle of the Ediacaran Period. A microfossil analysis of sediments from the upper parts of the Hailuoto Formation by Tynni & Donner (1980) drew comparisons with the uppermost parts of the Visingsö Formation of Sweden. Detrital zircon U–Pb ages have subsequently constrained the Visingsö Formation to a maximum depositional age of  $\leq 886 \pm 9$  Ma (Moczyłowska *et al.* 2017), and recent microfossil studies also suggest this formation was deposited during the Tonian (Loron & Moczyłowska, 2018). Klein *et al.* (2015), however, point out that many of the form-taxa reported from the Hailuoto Formation by Tynni & Donner (1980) are actually found in much younger sediments elsewhere in the Baltic region and East European Platform, for example, in late Ediacaran strata from the Kotlin Formation of Estonia (Mens & Pirrus, 1997; Meidla, 2017; Arvestål & Willman, 2020; Slater *et al.* 2020). A particularly close comparison can also be drawn with OWM assemblages from the late Ediacaran Redkino and Kotlin regional stages of the Lyamtsa, Verkhovka, Zimmie Gory and Yorga formations of the White Sea region in Russia (e.g. Leonov & Ragozina, 2007). These similarities to assemblages from comparatively well-constrained late Ediacaran strata (e.g. in the White Sea region) would suggest a substantially younger age for the Hailuoto Formation than suggested in previous studies, closer to the Ediacaran–Cambrian boundary. Indeed, U–Pb zircon dating of volcanic tuffs has indicated an age of 551–548 Ma for the lowermost Kotlin in the White Sea area of northern Russia (Grazhdankin *et al.* 2011). With this advancement in understanding of the local and regional stratigraphy we favour a younger, latest Ediacaran age for the upper part of the Hailuoto Formation here.

Another subsurface remnant of comparable Neoproterozoic sediments is preserved within the Saarijärvi impact structure in central Finland (Fig. 1). The Saarijärvi impact crater is situated 30 km south of Taivalkoski near the border between the Finnish regions of northern Ostrobothnia and Kainuu, and is largely covered by a lake (Saarijärvi) that has formed in the crater depression (to avoid confusion, it is worth noting that in Finnish ‘Saarijärvi’ is a very common lake name – there are at least 198

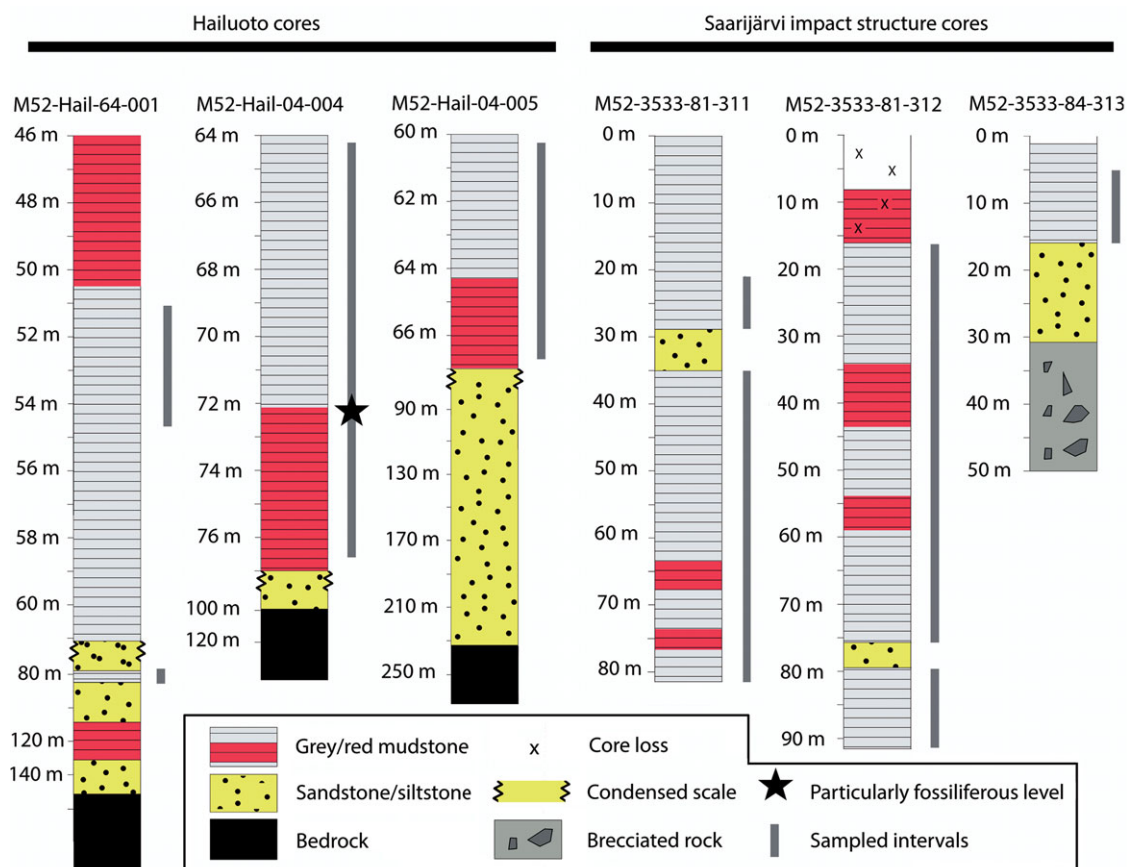


**Fig. 2.** (Colour online) Simplified stratigraphic sections of cores highlighting the major lithological changes and units. Grey bars represent sampled horizons, with sampling spaced at c. 1 m intervals, with denser sampling among finer-grained mudstones. Hailuoto sections are described in further detail in figures 10, 25 and 36 in Solismaa (2008).

lakes named Saarijärvi in Finland). The local geology has largely been reconstructed based on drillcore material. As with many impact structures, the precise geological history has been problematic to disentangle. Up to 156 m thickness of sediments is preserved within the ~1.5 km diameter crater. These packages of sediment are difficult to correlate even between closely spaced cores, likely as a result of separate cores intersecting different coherent megablocks of sediment arranged in a chaotic way (Hyypä & Pekkala, 1987; Öhman & Preeden, 2013). The signatures of impact-disruption are evident throughout the cores: Sediments display significant changes in dip direction and angle over relatively short intervals of core depth. Further, fractured angular clasts of basement rock (granite) are found within the sediments at several depths in different cores. Another notable feature is that even among soft lithologies the core material tends to break along shiny, polished surfaces which cut across the bedding; such features may represent subsequent fracturing of the sediments related to tectonism (Öhman & Preeden, 2013). Precise dating of the impact event has been difficult, and there are competing scenarios between a Proterozoic and an early Cambrian age impact hypothesis (see Öhman & Preeden, 2013). Shales and siltstones in the upper parts of the Saarijärvi impact structure are reminiscent of those in the Hailuoto Formation, and have produced comparable OWM assemblages both in terms of taxonomic composition and preservation (Tynni & Donner, 1980; Tynni & Uutela, 1984, 1985; Paulamäki & Kuivamäki, 2006), suggesting that sediments of the Hailuoto Formation originally extended north and east to cover a substantial portion of central Finland.

### 3. Materials and methods

Sampling targeted three cores intersecting the Neoproterozoic sediments of Hailuoto Island: M52-Hail-04-004 (drilled at an angle of 70° towards 226° direction), M52-Hail-04-005 and M52-Hail-64-001 (Fig. 1). In all cases our samples are derived from the green-grey and grey-brown mudstones which make up the upper parts of Hailuoto cores from 64–77 m depth of M52-Hail-04-004 (28 samples), 60–67 m depth of M52-Hail-04-005 (21 samples) and 75–80 m depth of M52-Hail-64-001 (5 samples) (Fig. 2; for additional details of cores see Solismaa, 2008). In addition, three cores intersecting the Saarijärvi impact crater were sampled: M52-3533-81-311, M52-3533-81-312 and M52-3533-84-313 (Figs 1, 2). These samples were also selected from green-grey mudrocks, which at Saarijärvi are distributed chaotically even among closely spaced cores, due to the displacement of megablocks associated with crater formation (see Öhman & Preeden, 2013). Processing followed the techniques outlined in Butterfield & Harvey (2012). Cores are housed at the Geological Survey of Finland national drillcore archive in Loppinen. All imaged fossil material is deposited in the Palaeontological collections of the Museum of Evolution (PMU), Uppsala University, Sweden.

### 4. Organic-walled fossils

Of the 64 processed samples, all were productive for microfossils, although with significant variation in contents and abundance. A particularly productive section was identified in mudstones of



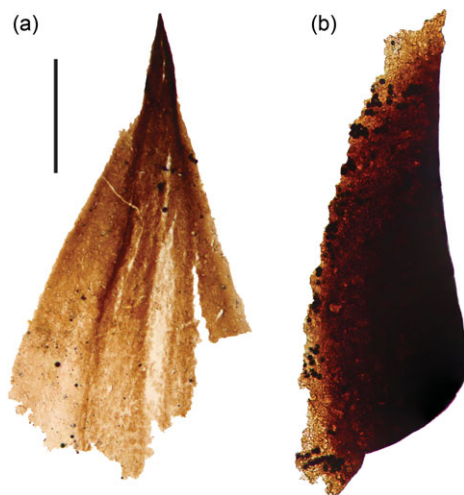


**Fig. 3.** (Colour online) Metazoan remains. (a) Sclerite likely derived from a bilaterian-grade metazoan. (b) Possible metazoan-derived serrated structure. Scale bar represents 200  $\mu\text{m}$ . (a) 72.70 m M52-Hail-04-004 core; (b) 72.2 m M52-Hail-04-004 core. Specimen numbers: (a) PMU 38-156/1; (b) 38-157/1.

the M52-Hail-04-004 drillcore, spanning ~71–73 m depth. The majority of recovered fossils fall into the broad form-taxonomic distinctions of acritarchs (vesicular organic-walled microfossils of unknown biological affinity; Evitt, 1963) or filamentous forms. Specimens of metazoan origin were also recovered from Hailuoto. Assemblages from Hailuoto and Saarijärvi contained the same acritarchs and filamentous form taxa, supporting previous hypotheses that these strata are remnants of once widespread late Ediacaran deposits in Finland (Tynni & Donner, 1980; Tynni & Uutela, 1985; Paulamäki & Kuivamäki 2006).

#### 4.a. Metazoan remains

An individual triangular structure of ~800  $\mu\text{m}$  length and ~450  $\mu\text{m}$  width at the base was recovered from a particularly fossil-rich sample at 72.7 m depth in the M52-Hail-04-004 drillcore. This spine-shaped fossil possesses a thin-walled flared basal region exhibiting rhombus-shaped surficial scaly ornamentation, which tapers to a darkened, presumably sclerotized tip (Fig. 3a). The same sample also produced a broadly blade-shaped sclerotized element edged with crenate serrations that are densely encrusted with pyrite euhedra (Fig. 3b).

Close comparisons can be drawn between the spine-shaped element (Fig. 3a) and early Cambrian carbonaceous ‘protoconodont’ spines (see *Protohertzina compressa*, figs 3, 4 of Slater *et al.* 2018a; fig. 3 of Slater & Willman, 2019). In particular, the tip closely resembles known early Cambrian spines of this type (compare to holotype specimen of *P. compressa*, fig. 3BA of Slater *et al.* 2018a). The basal portion of the Hailuoto spine, however, differs from these protoconodont-type spines: *P. compressa* exhibit a dense fibrous microstructure, whereas the Hailuoto spine displays a faint scaly ornament on an otherwise smooth basal portion. Broadly comparable ornamentation occurs on the basal pad of cuticular sclerites of scalidophoran worms (notably the triangular ‘teeth’ borne on the pharynx of such worms; see fig. 9K of Smith *et al.* 2015; fig. 3B of Slater *et al.* 2018b; fig. 2R of Wallet *et al.* 2021).

This spine is perhaps the most unexpected find from the Hailuoto assemblage, and appears to derive from a metazoan. Several Ediacaran metazoans (e.g. *Dickinsonia*, *Yorgia* and *Kimberella*) are known to have produced dorsal integumentary

shields that were covered with various tubercles and spines (see Ivantsov *et al.* 2019a, figs 2, 3). The fine-scale structures of these integuments are unclear however, since they are known solely from preservation as casts and moulds. Cnidarians can possess a chitinous exoskeleton (Mendoza-Becerril *et al.* 2016), which conceivably could produce sclerite-like elements preservable as carbonaceous fossil remains. Fossil examples of early cnidarians with a chitinous exoskeleton include early Cambrian (Fortunian) coronate scyphozoans such as *Olivoooides* (Dong *et al.* 2013), *Quadrapyrgites* (Y Liu *et al.* 2014) and *Qinscyphus* (Liu *et al.* 2017), as well as possible Ediacaran cnidarians such as the tubular *Corumbella* (Warren *et al.* 2012). None of these, nor any other cnidarians we are aware of, produce spine-like sclerites, however, and we deem it likely the sclerite from Hailuoto is sourced from a bilaterian-grade animal. Among the bilateria, protoconodonts and scalidophorans both have fossil records extending to almost the base of the Cambrian (Kouchinsky *et al.* 2012; Slater *et al.* 2018a). Some of the earliest Cambrian, and even latest Ediacaran, burrows may have been produced by scalidophoran or cycloneurialian worms (see Kesidis *et al.* 2019). Based on the simple set of characters, however, this spine cannot confidently be attributed to either a protoconodont, or a cuticular sclerite of a scalidophoran worm. Indeed, spines of this type could conceivably be sourced from a much broader array of bilaterians, including various ecdysozoans, gastrotrichs (Rieger & Rieger, 1977), gnathiferans (Marlétaz *et al.* 2019), as well as stem-protostomes or even stem-bilaterians.

#### 4.b. Filamentous microfossils

Both the Hailuoto and Saarijärvi material produced a rich assortment of microfossils with a broadly filamentous construction, some of which may represent different life-cycle stages, or taphomorphs of the same organism. Structures such as simple multicellular filaments or coccoid cells have been repeatedly convergent in some clades over geological time (e.g. cyanobacteria: Dvořák *et al.* 2014; Butterfield, 2015b), meaning that assigning these fossils to a specific group is fraught with difficulty. To circumvent some of this phylogenetic ambiguity, we discuss these forms in terms of distinctive morphogroups and, where possible, use established form-taxonomic terminology, whilst drawing comparisons to useful fossil and extant analogues.

##### 4.b.1. *Siphonophycus* ‘donuts’

A ubiquitous constituent of fossiliferous samples is bundled filaments of the form-taxon *Siphonophycus* (Fig. 4). *Siphonophycus* are smooth-walled, unbranched, tubular filaments that lack septa or preserved cellular remains (Knoll *et al.* 1991). The *Siphonophycus* filaments from Finland are a few microns in thickness, and are often found bundled up into tight rings varying in size between 50 and 650  $\mu\text{m}$  in maximum diameter, often with a central hollow (ranging between absent and up to ~300  $\mu\text{m}$  diameter). These structures likely represent flattened *Nostoc*-ball-like masses of interwoven filaments (see Butterfield *et al.* 1994; Mollenhauer *et al.* 1999; Guiry & Guiry, 2008). The ‘donut-shaped’ (Fig. 4a–k, n, p, q) and more irregular agglomerations (Fig. 4l, m, o, s) possibly formed via the collapse of originally torus-shaped colonies, or alternatively the central hollow may represent the void left by a mucilage-filled interior space within an originally spherical colony. Though lacking an overall ring shape, bundled filaments described as *Polytrichoides lineatus* Hermann 1974 emend. (Hermann in Timofeev *et al.* 1976) exhibit similarities to the

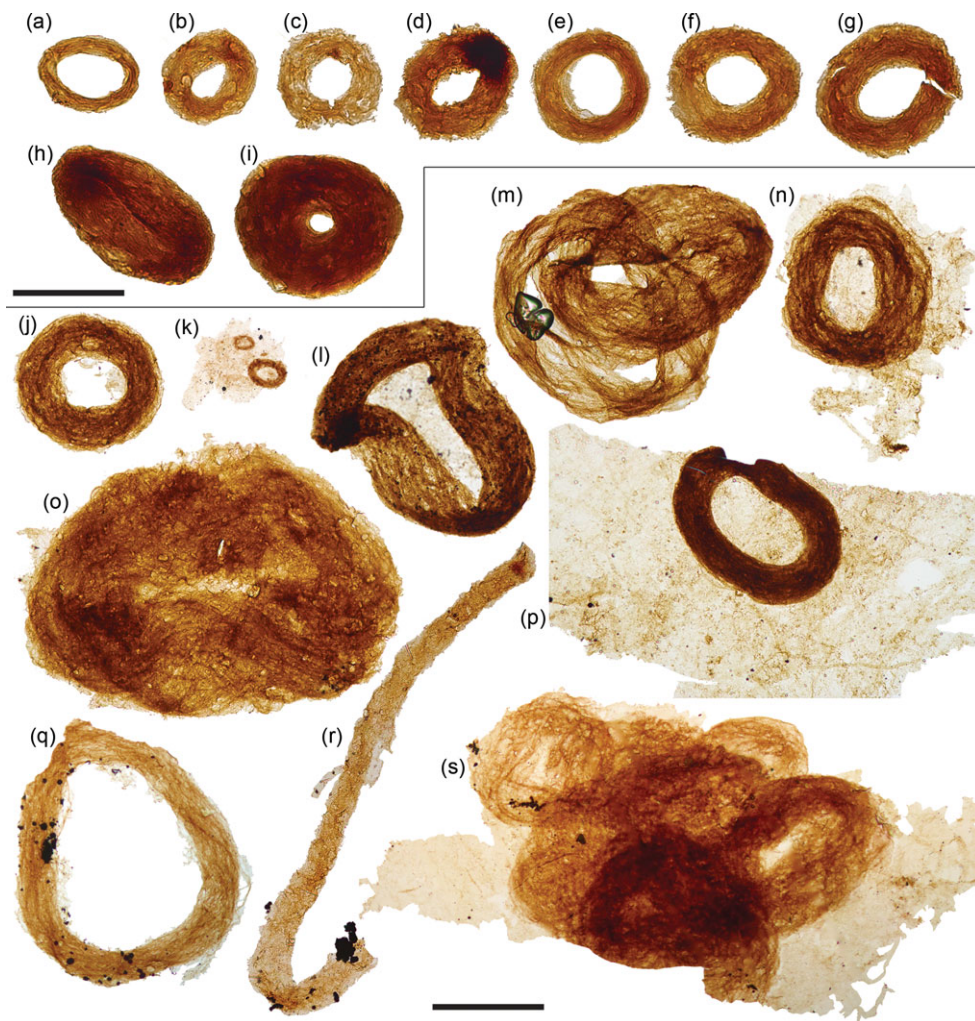


**Fig. 4.** (Colour online) *Siphonophycus* 'donuts'. (a–r) Bundled filaments of the form-taxon *Siphonophycus* forming 'donut-shaped' masses, possibly resulting from flattened *Nostoc*-ball-like masses of filaments. (k, m, s) Clusters of donut-shaped colonies. (k, n, p, s) Filament bundles adhered to broader, background mass of mat-like filamentous remains. (r) Broken loop. Scale bars represent 100  $\mu\text{m}$  (a–i); 200  $\mu\text{m}$  (j–s). (a, c, d) 7.53 m Saarijärvi M52/3533/84/313 core; (b, e, i) 20.20 m Saarijärvi M52/3533/81/312 core; (j, l–p, s) 72.2 m M52-Hail-04-004 core; (k, q, r) 72.70 m M52-Hail-04-004 core. All specimen numbers have the prefix PMU 38: (a) 165/6; (b) 166/6; (c) 165/7; (d) 165/8; (e) 166/1; (f) 166/2; (g) 166/3; (h) 166/4; (i) 166/5; (j) 158/1; (k) 159/1; (l) 157/2; (m) 157/3; (n) 158/2; (o) 158/3; (p) 158/4; (q) 160/1; (r) 161/1; (s) 162/1.

bundles of *Siphonophycus* described here, and are frequently recovered from Proterozoic assemblages (Li *et al.* 2019). A closer comparison comes from comparable tightly wound rings of filaments recorded from the Neoproterozoic Svanbergfjellet Formation of Spitsbergen (fig. 26G of Butterfield *et al.* 1994), suggesting this growth habit is widespread among Neoproterozoic cyanobacterial mats.

#### 4.b.2. *Palaeolyngbya*

The majority of samples produced smooth, strap-shaped filamentous sheaths, ranging between ~50 and 110  $\mu\text{m}$  in diameter, and of various lengths up to ~3 mm (Fig. 5). In a subset of these filaments, the outer envelopes enclose optically darker, unbranched, uniseriate, multicellular trichomes, composed of shrunken and degraded cells (Fig. 5m–p, x, ac, an). The trichome is *c.* 30–40 % of the outer envelope diameter in most specimens, though this may represent taphonomic shrinkage since a few specimens preserve much broader trichomes (e.g. Fig. 5x). The internal trichome may run the entire filament length (e.g. Fig. 5o); however, in some specimens it is fragmented or incomplete (e.g. Fig. 5p). The cells of

the trichome are occasionally separated and displaced obliquely within the sheath, appearing as a series of discoidal cells (e.g. Fig. 5ac). These filaments can be ascribed to the form-taxon *Palaeolyngbya* Schopf 1968 emend. Butterfield, Knoll and Swett 1994 (see pl. 2, fig. 1 of Yun, 1981; fig. 2.1 of Vidal & Moczyłowska, 1992; fig. 25E–G of Butterfield *et al.* 1994; figs 4–5 of Moczyłowska, 2008; fig. 3J of Loron *et al.* 2019; fig. 100–X of Arvestål & Willman, 2020). These filaments are distinguishable from other fossil multicellular trichomes such as *Oscillatorioopsis* from the manner in which specimens break (across pseudosepta vs between true cells in *Oscillatorioopsis*). Occasional specimens display a pseudoseptate sheath comparable to some *Tortunema* (e.g. fig. 7.5 of Sergeev *et al.* 2016), likely reflecting taphomorphic and/or ontogenetic variation.

#### 4.b.3. *Rugosoopsis*

Another common filament type found in most samples from Hailuoto and Saarijärvi consists of a bi-layered form with a dense, smooth-walled inner sheath (similar to *Siphonophycus* or *Palaeolyngbya*), enclosed by a thinner-walled outer sheath with



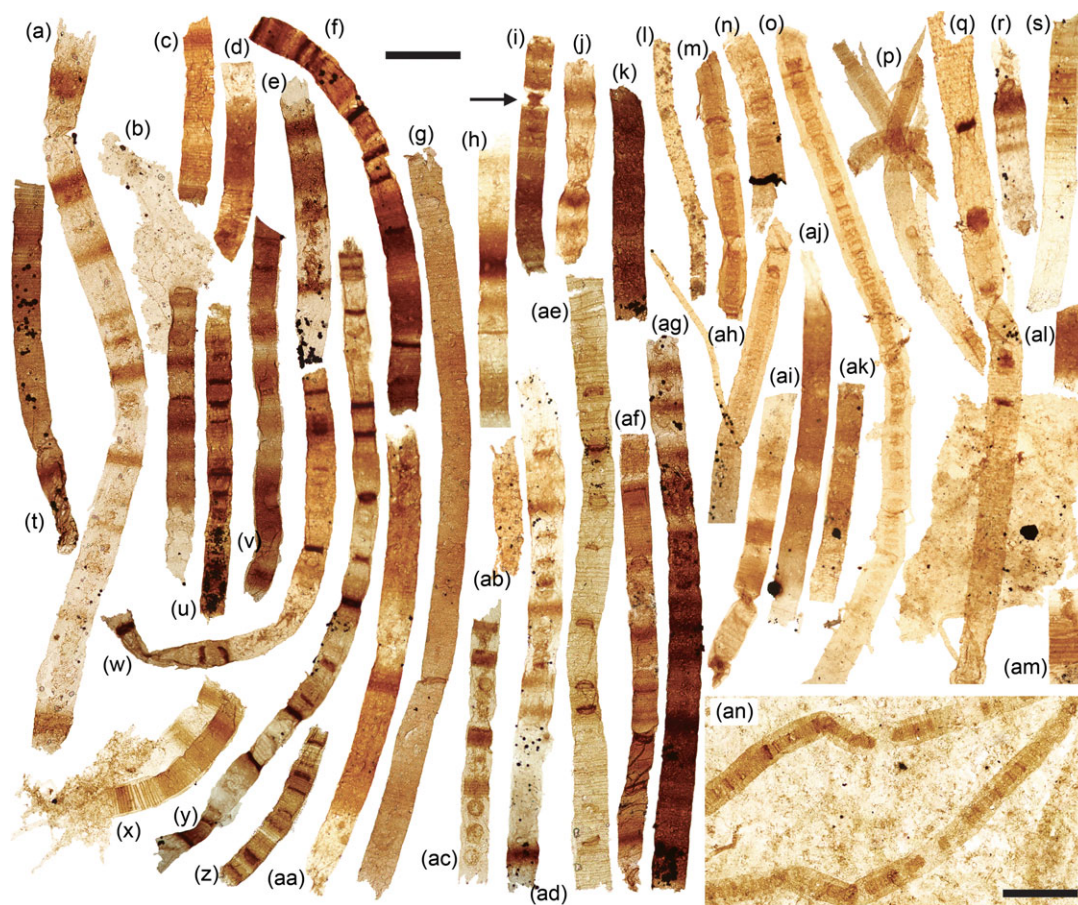


**Fig. 5.** (Colour online) Filamentous microfossils. (a–l, r–w, y–ab, af–am) *Rugosoopsis*. (m–p, x, ac, an) *Palaeolyngbya*. (q, ad, ae) Exhibit mixed morphology of *Rugosoopsis*-like filaments with occasional lengths of *Palaeolyngbya*-like trichome. (an) *Palaeolyngbya* filaments adhered to matted sheet of filamentous remains. Arrow indicates shrivelled cell (necridia) in specimen (i). Note the discoidal cells of the trichome in (r), (ac) and (ae). Scale bars represent 200  $\mu\text{m}$ . (a–l, n, r–t, w), y–ab, ad, af, ag, ai–am) 72.70 m M52-Hail-04-004 core; (m, o–q, u, v, x, ac, ae, ah, an) 72.20 m M52-Hail-04-004 core. All specimen numbers have the prefix PMU 38: (a) 161/2; (b) 161/3; (c) 161/4; (d) 163/1; (e) 161/5; (f) 156/2; (g) 161/6; (h) 160/2; (i) 160/3; (j) 159/2; (k) 161/7; (l) 161/12; (m) 162/2; (n) 159/3; (o) 162/3; (p) 162/4; (q) 162/5; (r) 159/4; (s) 160/4; (t) 161/8; (u) 158/5; (v) 157/4; (w) 156/3; (x) 157/5; (y) 160/5; (z) 164/4; (aa) 160/6; (ab) 161/9; (ac) 157/6; (ad) 160/7; (ae) 158/6; (af) 161/10; (ag) 161/11; (ah) 162/6; (ai) 163/2; (aj) 163/3; (ak) 159/5; (al) 163/4; (am) 163/5; (an) 157/7.

a pronounced series of transverse ridges (or rugose ornamentation) on the surface (Figs 5a–l, r–w, y–ab, af–am, 6d). The broader outer sheath is often damaged or torn, but where intact it appears as a faint outline extending beyond the margins of the inner sheath (Fig. v, y, z). Occasional atrophied cells (probable necridia) are visible within the inner sheath (e.g. Fig. 5i). These filaments are assignable to the form-taxon *Rugosoopsis* Timofeev and Hermann 1979, which has been recovered from Proterozoic shales (Pjatiletov, 1988; Jankauskas *et al.* 1989; fig. 25A–D of Butterfield *et al.* 1994; fig. 3 of Samuelsson & Butterfield 2001; fig. 10.1 of Sergeev *et al.* 2011; fig. 2J, T of Riedman *et al.* 2014; fig. 15.13 of Riedman & Porter, 2016) and as silicified three-dimensional fossils within Proterozoic shallow water carbonates (fig. 9F–I of Butterfield, 2001). In both the Hailuoto and Saarijärvi samples, these *Rugosoopsis* filaments co-occur with and may grade into other filament types, including *Palaeolyngbya*, *Siphonophycus* and occasional pseudoseptate *Tortunema*-like sheaths (Fig. 4q, ad, ae), underscoring the substantial taphomorphic and ontogenetic overlap among filamentous microfossils.

#### 4.b.4. *Obruchevella*

Abundant coiled, thin-walled filaments (~10–20  $\mu\text{m}$  in diameter) occasionally with apparent septa were recovered in all samples

from Hailuoto and Saarijärvi (Figs 7f, 8h–n). The majority of specimens are compressed into a coiled ring, but occasional specimens show laterally displaced coils (Fig. 7f, 8i, l), revealing a *Spirulina*-like helical habit (see Sili *et al.* 2012). Compressed cylindrical forms were recovered in previous investigations by Tynni & Donner (1980), who assigned these to the form-taxon *Volyniella cylindrica* (compare also with fig. 1F of Leonov & Ragozina, 2007; figs 3, 5 of Sharma & Shukla, 2012). Jankauskas *et al.* (1989) point out that the distinction between the flattened, two-dimensional *Volyniella* (Shepeleva, 1973) and typically three-dimensionally preserved *Obruchevella* (e.g. Anderson *et al.* 2018; Willman *et al.* 2020) is essentially artificial, and based on taphomorphs. Noting that there are several possible names for spiralled filaments (in addition to *Volyniella*, also *Glomovertella* and *Circumiella*), we prefer to follow the recommendations of Jankauskas *et al.* (1989) and term these coiled filaments *Obruchevella*.

#### 4.b.5. Matted filaments

The majority of samples produced abundant entangled mats of *Siphonophycus*, *Palaeolyngbya* and *Rugosoopsis* exhibiting a mesh-like growth habit (Figs 6, 7), where filaments are densely interwoven (Figs 6a–d, 7a). Frequently the density of overlapping filaments is such that they form a sheet-like layer that has been

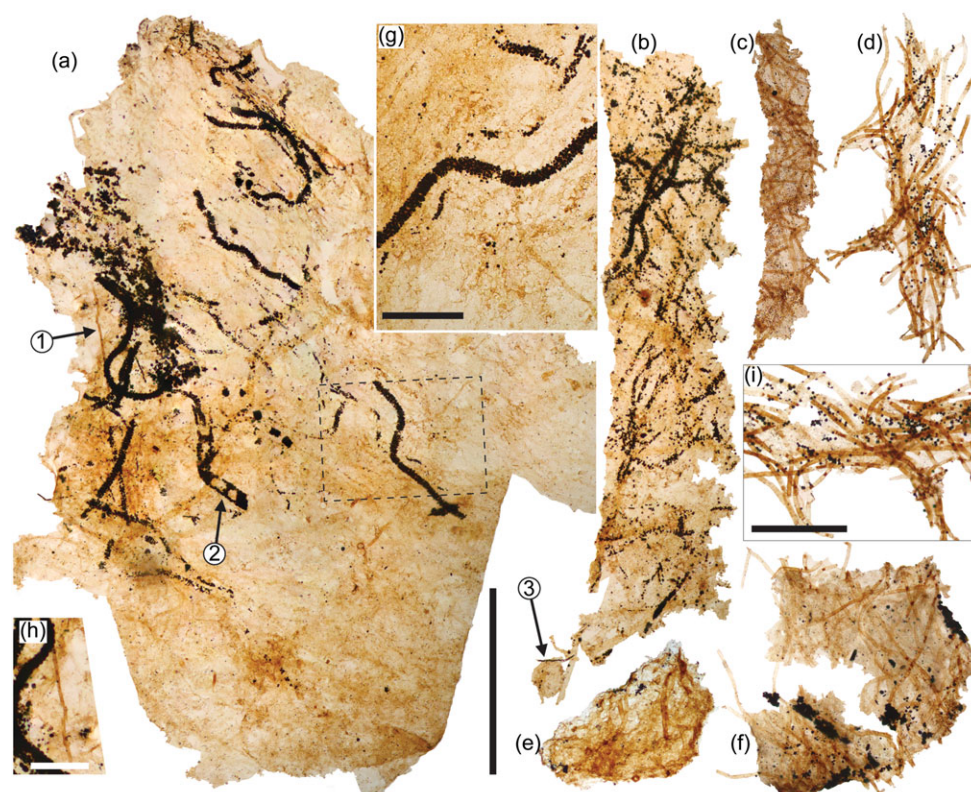


**Fig. 6.** (Colour online) Matted filaments. (a, b) Large sheets of matted filaments where many of the broader filaments are outlined in dense encrustations of pyrite euhedra. (c) Interwoven *Siphonophycus* filaments. (d) Tangled mass of *Rugosoopsis* filaments. (e, f) Interwoven masses of fine 'hyphae-like' filaments. (g) Enlargement of area inside dashed box in specimen (a) showing filament outlined by pyrite euhedra. (h) Enlargement of fine filament in specimen (a) indicated by arrow 1. (i) Enlargement of filaments in (d) showing prominent shrivelled necridia. Pyrite outlining apparent cells or septa (arrow 2). A variety of organic walled microfossils can be found among these matted filaments (e.g. leiosphaerid acritarch entangled with filaments; arrow 3). Scale bars represent 0.5 mm (a–f), 100  $\mu$ m (g, h), 200  $\mu$ m (i). (a, b, g, h) 72.20 m M52-Hail-04-004 core; (c–f, i) 72.70 m M52-Hail-04-004 core. All specimen numbers have the prefix PMU 38: (a, g, h) 162/7; (b) 162/8; (c) 164/1; (d) 1, 163/6; (e) 160/8; (f) 159/6.

compressed into a single carbonaceous film (see Martí Mus, 2014; Slater *et al.* 2020). Some of these mats are of mixed composition (e.g. Fig. 6a); however, others are composed entirely from a single filament morphology (e.g. Figs 6c, d, 7a). In this latter category, the filaments are all of similar dimensions, suggesting that they are at the same ontogenetic stage (e.g. Fig. 7a). Within these mats, individual filamentous structures may be encrusted with pyrite euhedra (Figs 6a, b, 7c, e). Pyrite also occurs as circular or more irregular patches within the sheet, possibly representing voids within the mat created by gas bubbles. Together, these agglomerations are reminiscent of various acid-isolated mat-forming filaments from Proterozoic shales (compare Fig. 6c with fig. 8.5 of Sergeev *et al.* 2016; fig. 2 of Samuelsson & Butterfield, 2001; fig. 2G of Butterfield, 2015a; fig. 4D of Butterfield, 2015b) and carbonates (Knoll *et al.* 2013).

#### 4.c. Acritarchs

The majority of samples from both Hailuoto and Saarijärvi produced irregular, aggregate clusters of spheroids (Fig. 9m, n). Comparable sheet-forming clusters of spheroids are frequently assigned to the form-taxon *Ostiana* (e.g. fig. 5J of Samuelsson & Butterfield, 2001); however, the more irregular aggregates recovered here are more appropriately assigned to the form-taxon *Synsphaeridium* Eisenack 1965 (Fig. 9m, n; cf. fig. 13 of Riedman & Porter, 2016). The individual spheroids range between

15 and 25  $\mu$ m in diameter, and form clusters up to ~350  $\mu$ m in maximum dimension, consisting of up to ~100 individual spheroids. More tightly bound and regular-shaped clusters of spheroids (e.g. Fig. 9j–l), where the vesicles are often deformed by compression, are assigned to *Symplastosphaeridium* Timofeev 1959, 1966 (cf. fig. 18.6 of Hofmann & Jackson, 1994). Occasionally, similar forms have been ascribed to *Squamosphaera colonialica* Jankauskas 1979, but *Squamosphaera* do not possess true vesicles, displaying only hemispherical protrusions from the vesicle wall (see fig. 17 of Porter & Riedman, 2016).

Larger cell-aggregates with denser walls were found in most samples, but were particularly abundant in samples from Hailuoto (Fig. 9e–h). Fragmentary forms of identical morphology to these acritarchs were described by Tynni & Donner (1980) from the same sediments on Hailuoto, which they ascribed to the extant prasinophycean alga genera *Cymatiosphaera* as a new species, *Cymatiosphaera precamblica* (a holotype was not formally designated in that paper, but was rectified in Tynni & Donner, 1982). Tynni & Donner (1980) extrapolated the size of the fragmentary remains to be derived from a spherical body *c.* 250  $\mu$ m in diameter when complete; this falls towards the lower end of the size range of forms recovered in this study (~300–700  $\mu$ m), perhaps reflecting the differing processing techniques. Assignment of fossil material to the extant genus *Cymatiosphaera* is not unknown (e.g. *Cymatiosphaera* are reported from the Early Devonian Rhynie Chert; Dotzler *et al.* 2007). However, the surface sculpture



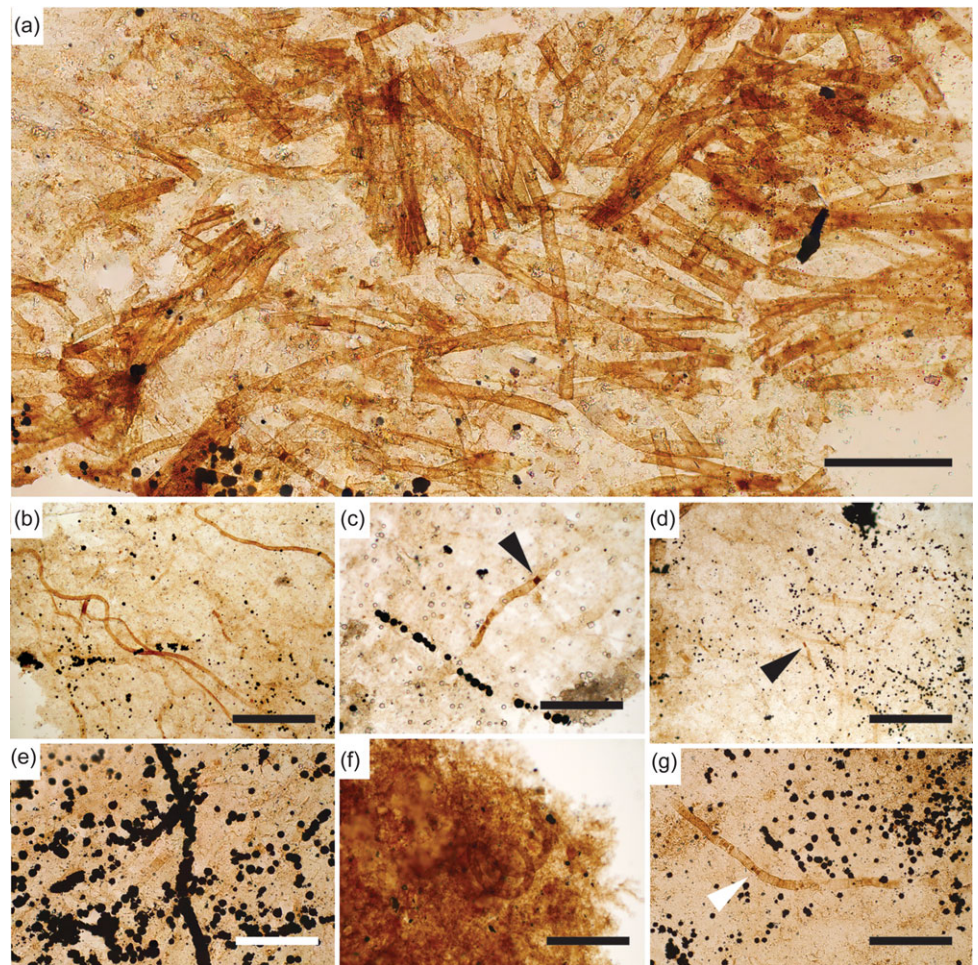


**Fig. 7.** (Colour online) Matted filaments. (a) Interwoven filamentous mat. (b) Sinuous ribbon-like filaments on surface of mat, alongside chain of pyritized trichome. (c) Mixture of *Siphonophycus*, *Rugosoopsis* and pyrite-encrusted filaments (arrow points to necridia within *Rugosoopsis*-type filament). (d) Dense mat of *Rugosoopsis* exhibiting pyrite encrustation (arrow points to prominent necridia). (e) Pyrite-encrusted filaments. (f) Coiled *Obruchevella*-type filament within mat. (g) Degraded mat with prominent *Rugosoopsis* filament (white arrow points to necridia). Scale bars represent 200  $\mu\text{m}$  (a, b, d); 100  $\mu\text{m}$  (c, e–g). (a–g) 72.70 m M52-Hail-04-004 core. All specimen numbers have the prefix PMU 38: (a) 164/5; (b) 163/7; (c) 163/8; (d) 163/9; (e) 164/2; (f) 163/10; (g) 164/3.

of specimens recovered by Tynni & Donner (1980) was originally interpreted as reticulate, as in extant *Cymatiosphaera*. Our recovery of intact specimens here nevertheless demonstrates that the apparently polygonal surface texture actually results from the intersection of compacted adjacent spheroids, which clearly protrude at the flattened cluster margins (Fig. 9e–h). In light of this, these densely clustered cell aggregates are instead more appropriately compared to cell colonies found within organic cysts such as those reported in some *Chuar* (see fig. 3 of Tang *et al.* 2017).

Acritarchs assigned to *Chuar* were found to co-occur with these large cell-aggregate forms (Fig. 9a–b). Feasibly, the large cell aggregates represent the vegetative stage of co-occurring empty *Chuar* cysts. Tang *et al.* (2017) suggest that although these cell aggregates could be described under a distinct form-taxonomic name, they likely represent different life-cycle stages of the same biological species, and therefore it may be suitable to expand the form taxonomy of *Chuar* to encompass these aggregate forms (see also *Chuar* as a subcomponent of a macroalgae, fig. 16 of Kumar, 2001; fig. 7 of Wang *et al.* 2017). Less optically dense forms could potentially fall under the definition of *Leiosphaeridia jacutica* (see Javaux & Knoll, 2017). Other hollow cyst-like acritarchs recovered include relatively large smooth-walled *Leiosphaeridia* (Fig. 9c) with prominent compaction folds encrusted in pyrite (compare with fig. 1 of Slater & Budd, 2019).

## 5. Discussion

### 5.a. Palaeoenvironment of Hailuoto/Saarijärvi OWM assemblage

As with most assemblages of acid-extracted organic-walled fossils, the Hailuoto and Saarijärvi material likely represents a combination of both benthic and planktonic organisms. Smaller vesicular acritarchs may be sourced from the water column, whereas the majority of the filamentous taxa appear to be benthic, based on their mat-forming interwoven habit. Indeed, OWM assemblages from mid- to late-Proterozoic siliciclastic sediments record a prevalence of mat-forming filaments in shallow-water assemblages, probably reflecting photic-zone colonization by cyanobacterial mats (Butterfield & Rainbird, 1998; figs 6, 7 of Butterfield & Chandler, 1992; Butterfield, 2015b). Filamentous bacterial mats can nevertheless form at a wide range of depths on modern sea-floors; whilst shallow-water mats tend to be principally composed of cyanobacteria, deeper water mats are frequently dominated by filamentous sulphur-oxidizing bacteria (Williams & Reimers, 1983; Jannasch *et al.* 1989; Bernard & Fenchel, 1995). Despite the inherent difficulties of determining the phylogenetic affinities of simple fossil filaments, there is a case for viewing the filamentous mats at Hailuoto and Saarijärvi as largely cyanobacterial; matted sheaths of *Palaeolyngbya* and *Rugosoopsis* share a number of



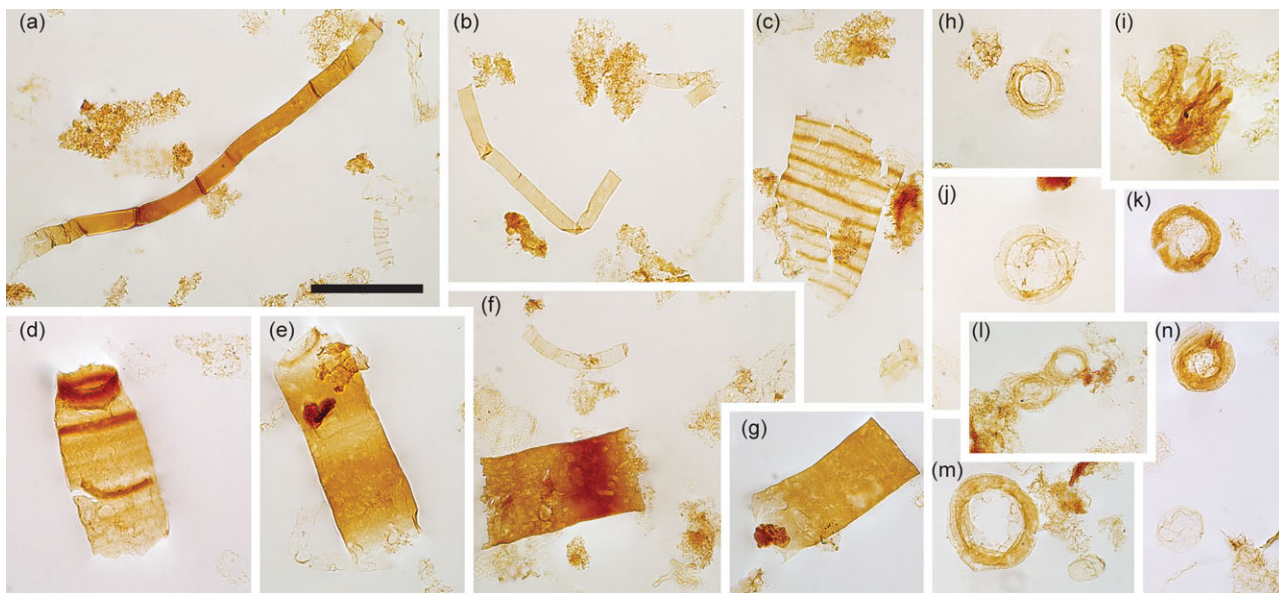


**Fig. 8.** (Colour online) Filaments and acritarchs (small). (a–b) Smooth sheaths of *Siphonophycus*. (c) Possible fragment of *Cephalonyx*-type filament showing regular transverse banding. (d–g) Typical fragments of *Rugosoopsis*. (h–n) Specimens of *Obruchevela*, comprising chains of cell rings. (l, l) Show laterally displaced rings. Scale bar represents 100 μm. (a–n) 7.53 m Saarijärvi M52/3533/84/313 core. All specimen numbers have the prefix PMU 38: (a) 165/9; (b) 165/10; (c) 165/11; (d) 165/12; (e) 165/13; (f) 165/14; (g) 165/15; (h) 165/16; (i) 165/17; (j) 165/18; (k) 165/19; (l) 165/20; (m) 165/21; (n) 165/22.

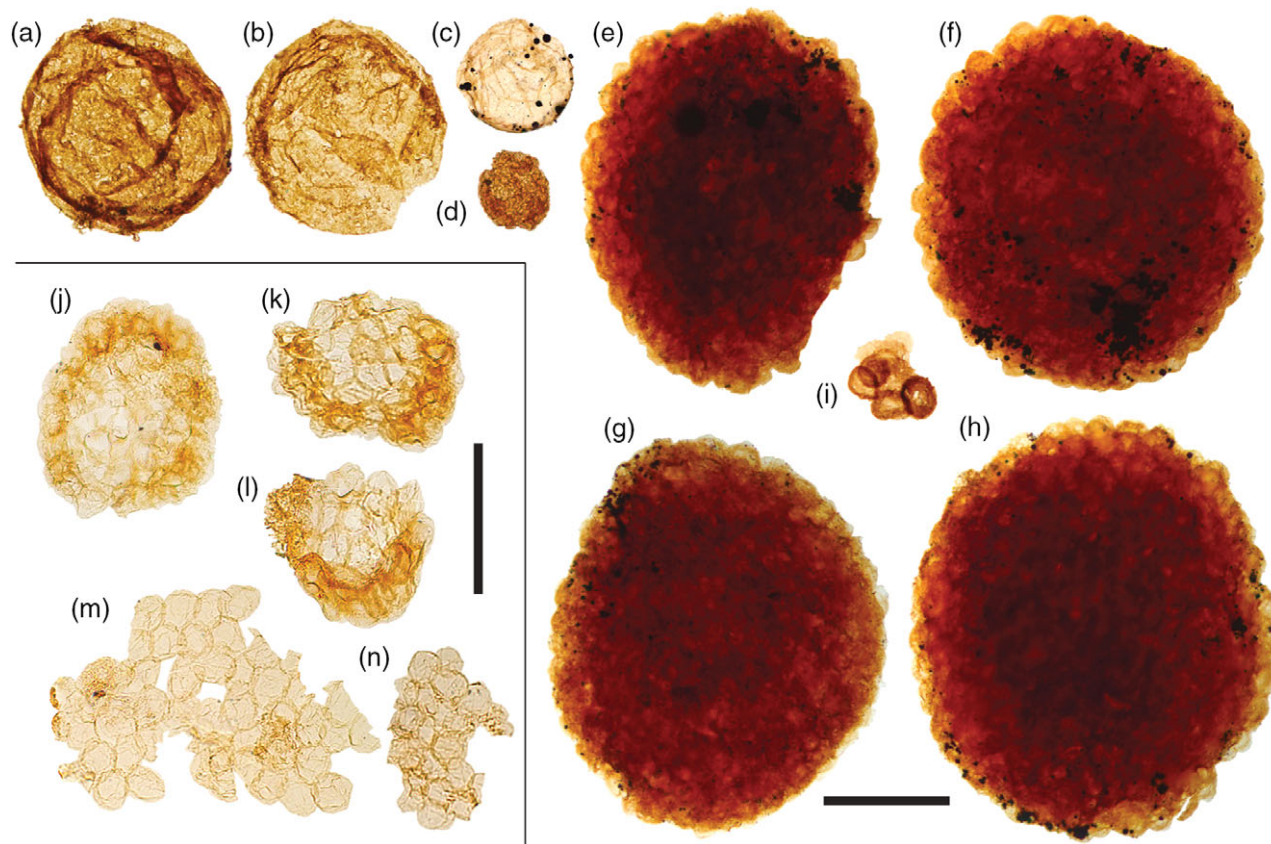


**Fig. 9.** (Colour online) Acritarchs (large). (a, b) *Chuaria* sp. (c) Large leiosphaerid encrusted with pyrite framboids. (d) Cell aggregate mass. (e–h) Large, densely packed cell aggregates. (i) Cluster of sphaeromorphic acritarchs. (j–l) Compact, regular spheroid clusters assigned to *Symplassosphaeridium*. (m, n) Irregular aggregates of loosely-bound spheroids assigned to *Synsphaeridium*. Scale bars represent 200 μm (a–i); 100 μm (j–n). (a, b, i) 72.20 m M52-Hail-04-004 core; (c–h) 72.70 m M52-Hail-04-004 core; (j–n) 7.53 m Saarijärvi M52/3533/84/313 core. All specimen numbers have the prefix PMU 38: (a) 158/7; (b) 157/8; (c) 159/7; (d) 161/13; (e) 156/4; (f) 156/5; (g) 160/9; (h) 160/10; (i) 162/9; (j) 165/1; (k) 165/2; (l) 165/3; (m) 165/4; (n) 165/5.

features with the extant cyanobacteria *Oscillatoria*, *Calothrix* and *Lyngbya*; for example, lengths of *Rugosopsis* are divided into a trichome and tend to break around shrivelled portions which potentially represent necridia – features associated with oscillatoriacean cyanobacteria (Lamont, 1969; Speziale & Dyck, 1992; Butterfield *et al.* 1994; Samuelsson & Butterfield, 2001). The cells of the trichome in *Palaeolyngbya* also occur as a series of stacked discs, and exhibit features resembling hormocyte cells (compare Fig. 5ac with fig. 2D of Curren & Leong, 2018) as in extant *Oscillatoria* and *Lyngbya* (Shukovsky & Halfen, 1976; Horodyski, 1977; Nagarkar, 2002; Rani *et al.* 2016). Cyanobacterial mats would support a shallow-water depositional environment for the sequences at Hailuoto/Saarijärvi (Tynni & Donner, 1980; Kohonen & Rämö, 2005), although even within the photic zone such mats are likely to include a variety of other microbes (Grazhdankin & Gerdes, 2007; Davies *et al.* 2016). Other probable benthic elements among the Hailuoto/Saarijärvi assemblages include a subset of the larger vesicular acritarchs (*sensu* Butterfield 2005, 2007; Knoll *et al.* 2006), and donut-shaped rings of *Siphonophycus* that probably grew as spherical nostocalean-like cyanobacterial colonies on late Ediacaran seafloors (see extant *Nostoc*; Mollenhauer *et al.* 1999). Larger versions of these colonies may be responsible for Ediacaran microfossils such as *Beltanelliformis* (Steiner & Reitner, 2001; Bobrovskiy *et al.* 2018b), or even certain *Aspidella* and torus-shaped structures on the surface of Ediacaran microbial mats (e.g. Dzaugis *et al.* 2018).

### 5.b. Ediacaran microbial mats and bilaterians

Trace fossil assemblages in terminal Ediacaran (c. 555–541 Ma) sediments (globally) contain burrows that appear to have been produced by animals with a coelom/hydrostatic internal cavity and an anterior concentration of sensory systems (Budd & Jensen, 2000), meaning that at least stem-grade bilaterians were present in benthic communities by this time (e.g. Jensen *et al.* 2000, 2006; Jensen, 2003; Narbonne, 2005; Chen *et al.* 2013; Schiffbauer *et al.* 2016; Herringshaw *et al.* 2017; Laing *et al.* 2019; Davies *et al.* 2020). The cuticular fragments recovered at Hailuoto (Fig. 3) demonstrate that body-fossil remains of such bilaterian-grade animals are preserved not only in the Phanerozoic but also in the Ediacaran SCF record. This raises the significance of these otherwise predominantly prokaryotic microbial mat-type fossil assemblages; given the central importance of bilaterians in shaping the nature of the Phanerozoic biosphere, the environment(s) and ecological backdrop of early bilaterian evolution are of intense palaeobiological interest (Budd & Jensen, 2017).

A variety of macroscopic surface textures on Ediacaran bedding planes have been attributed to microbial mats, often termed microbially induced sedimentary structures or ‘MISS’ (see a review of such structures in Davies *et al.* 2016). Microbial mats have also been widely invoked in the preservation of Ediacaran mouldic microfossils (e.g. Gehling, 1999; Gehling & Droser, 2009; but see Bobrovskiy *et al.* 2019 for an alternative view). In the latter part of the Ediacaran, bedding planes exhibiting MISS are frequently associated with simple horizontal burrows (e.g. Chen *et al.* 2013). This association has led to the hypothesis that Ediacaran bilaterians exploited such matgrounds as sources of nutrient concentration (Stanley, 1973; Seilacher 1999; Jensen *et al.* 2005; Seilacher *et al.* 2005; Buatois *et al.* 2011; Gingras *et al.* 2011; Meyer *et al.* 2014; Evans *et al.* 2019; Ivantsov *et al.* 2019b), or as oxygen-rich microenvironments if photosynthetic (Canfield & Des Marais, 1993; McIlroy & Logan 1999; Gingras *et al.* 2011; Ding *et al.* 2019). Current accounts of Ediacaran matground

habitats are almost entirely based on records from MISS, cast-and-mould fossils and trace fossils. Steiner & Reitner (2001) reported carbonaceous compressions of macroscopic Ediacaran taxa from the White Sea region; associated with these fossils were bedding-plane visible ‘elephant skin’ and wrinkle structures attributed to microbial mat imparted textures. Acid treatment was shown to produce *Siphonophycus* and other filamentous sheaths comparable to those recovered from Hailuoto and Saarijärvi (compare Figs 6–7 with fig. 6 of Steiner & Reitner, 2001), including pyritized sheaths similar to those reported here (see fig. 7 of Steiner & Reitner, 2001). Our data from the late Ediacaran of Finland demonstrate that such preservation is widespread, even in the absence of carbonaceous macrofossil preservation. In this light, SCF-style processing and investigation of late Ediacaran sediments can be viewed as a largely untapped taphonomic window, offering new insights into the critical change from matground to mixground seafloor environments as the Proterozoic gave way to the Phanerozoic.

## 6. Conclusions

Late Ediacaran sedimentary rocks from subsurface deposits in central Finland contain well-preserved carbonaceous microfossils, including an abundance of filamentous prokaryotes (probable cyanobacteria), a variety of acritarchs, and significantly, fragments of metazoan cuticle derived from bilaterians. Based on the composition of the recovered fossil assemblage, we revise previous interpretations of an early- to mid-Ediacaran age to a late Ediacaran age for the upper part of the Hailuoto Formation.

**Acknowledgements.** SW and BJS acknowledge joint first authorship of this paper. We thank Marko Puonti for help in collection of samples and logistical work at the Finnish national drillcore archive in Loppi, and Jussi Pokki (Geological Survey of Finland) for helpful advice. Insightful comments by Heda Agić (University of California, Santa Barbara) and an anonymous reviewer improved the manuscript. BJS acknowledges the support of Swedish Research Council (VR) grant 2020-03314.

## References

- Anderson RP, McMahon S, Macdonald FA, Jones DS and Briggs DEG (2018). Palaeobiology of latest Ediacaran phosphorites from the upper Khesen Formation, Khusvsugul Group, northern Mongolia. *Journal of Systematic Palaeontology* **17**, 501–32.
- Arvestål EHM and Willman S (2020) Organic-walled microfossils in the Ediacaran of Estonia: biodiversity on the East European platform. *Precambrian Research* **341**, 1–27.
- Bernard C and Fenchel T (1995) Mats of colourless sulphur bacteria. II. Structure, composition of biota and successional patterns. *Marine Ecology Progress Series* **128**, 171–9.
- Bobrovskiy I, Hope JM, Ivantsov A, Nettersheim BJ, Hallmann C and Brocks JJ (2018a) Ancient steroids establish the Ediacaran fossil Dickinsonia as one of the earliest animals. *Science* **361**, 1246–9.
- Bobrovskiy I, Hope JM, Krasnova A, Ivantsov A and Brocks JJ (2018b) Molecular fossils from organically preserved Ediacara biota reveal cyanobacterial origin for *Beltanelliformis*. *Nature Ecology & Evolution* **2**, 437–40.
- Bobrovskiy I, Krasnova A, Ivantsov A, Luzhnaya E and Brocks JJ (2019) Simple sediment rheology explains the Ediacara biota preservation. *Nature Ecology & Evolution* **3**, 582–9.
- Bogdanova SV, Bingen B, Gorbatshev R, Kheraskova TN, Kozlov VI, Puchkov VN and Volozh YA (2008) The East European Craton (Baltica) before and during the assembly of Rodinia. *Precambrian Research* **160**, 23–45.
- Buatois LA, Mángano MG, Noffke N and Chafetz H (2011) The trace-fossil record of organism-matground interactions in space and time. In *Microbial*



- Mats in Siliciclastic Sediments*. (eds N Noffke and H Chafetz), pp. 15–28. SEPM Special Publication 101.
- Buatois LA, Narbonne GM, Mángano MG, Carmona NB and Myrow P** (2014) Ediacaran matground ecology persisted into the earliest Cambrian. *Nature Communications* **5**, 3544.
- Budd GE** (2015) Early animal evolution and the origins of nervous systems. *Philosophical Transactions of the Royal Society B: Biological Sciences* **370**, 20150037.
- Budd GE and Jensen S** (2000) A critical reappraisal of the fossil record of the bilaterian phyla. *Biological Reviews* **75**, 253–95.
- Budd GE and Jensen S** (2017) The origin of the animals and a ‘Savannah’ hypothesis for early bilaterian evolution. *Biological Reviews* **92**, 446–73.
- Butterfield NJ** (2001) Paleobiology of the late Mesoproterozoic (ca. 1200 Ma) hunting formation, Somerset Island, arctic Canada. *Precambrian Research* **111**, 235–56.
- Butterfield NJ** (2005) Probable Proterozoic fungi. *Paleobiology* **31**, 165–82.
- Butterfield NJ** (2007) Macroevolution and macroecology through deep time. *Palaeontology* **50**, 41–55.
- Butterfield NJ** (2015a) The Neoproterozoic. *Current Biology* **25**, 859–63.
- Butterfield NJ** (2015b) Proterozoic photosynthesis – a critical review. *Palaeontology* **58**, 953–72.
- Butterfield NJ and Chandler FW** (1992) Palaeoenvironmental distribution of Proterozoic microfossils, with an example from the Agu Bay Formation, Baffin Island. *Palaeontology* **35**, 943–57.
- Butterfield NJ and Harvey THP** (2012) Small carbonaceous fossils (SCFs): a new measure of early Paleozoic paleobiology. *Geology* **40**, 71–4.
- Butterfield NJ, Knoll AH and Swett K** (1994) Paleobiology of the Neoproterozoic Svanbergfjellet Formation, Spitsbergen. *Fossils & Strata* **27**, 1–84.
- Butterfield NJ and Rainbird RH** (1998) Diverse organic-walled fossils, including “possible dinoflagellates”, from the early Neoproterozoic. *Geology* **26**, 963–6.
- Canfield DE and Des Marais DJ** (1993) Biogeochemical cycles of carbon, sulfur, and free oxygen in a microbial mat. *Geochimica Cosmochimica Acta* **57**, 3971–84.
- Chen Z, Zhou C, Meyer M, Xiang K, Schiffbauer JD, Yuan X and Xiao S** (2013) Trace fossil evidence for Ediacaran bilaterian animals with complex behaviors. *Precambrian Research* **224**, 690–701.
- Chen Z, Zhou C, Yuan X and Xiao S** (2019) Death march of a segmented and trilobate bilaterian elucidates early animal evolution. *Nature* **573**, 412–15.
- Curren E and Leong SCY** (2018) *Lyngbya regalis* sp. nov. (Oscillatoriales, Cyanophyceae), a new tropical marine cyanobacterium. *Phytotaxa* **367**, 120–32.
- Davies NS, Liu AG, Gibling MR and Miller RF** (2016) Resolving MISS conceptions and misconceptions: a geological approach to sedimentary surface textures generated by microbial and abiotic processes. *Earth-Science Reviews* **154**, 210–46.
- Davies NS, Shillito AP, Slater BJ, Liu AG and McMahon WJ** (2020) Evolutionary synchrony of Earth’s biosphere and sedimentary-stratigraphic record. *Earth-Science Reviews* **201**, 102979.
- Ding W, Dong L, Sun Y, Ma H, Xu Y, Yang R, Peng Y, Zhou C and Shen B** (2019) Early animal evolution and highly oxygenated seafloor niches hosted by microbial mats. *Scientific Reports* **9**, 1–11.
- Dong XP, Cunningham JA, Bengtson S, Thomas CW, Liu J, Stampanoni M and Donoghue PCJ** (2013) Embryos, polyps and medusae of the Early Cambrian scyphozoan *Olivoooides*. *Proceedings of the Royal Society B* **280**, 20130071.
- Dotzler N, Taylor TN and Krings M** (2007) A prasinophycean alga of the genus *Cymatiosphaera* in the Early Devonian Rhynie chert. *Review of Palaeobotany and Palynology* **147**, 106–11.
- Dvořák P, Casamatta DA, Pouličková A, Hašler P, Ondřej V and Sanges R** (2014) *Synechococcus*: 3 billion years of global dominance. *Molecular Ecology* **23**, 5538–51.
- Dzauigis PW, Evans SD, Droser ML, Gehling JG and Hughes IV** (2018) Stuck in the mat: *Obamus coronatus*, a new benthic organism from the Ediacara Member, Rawnsley Quartzite, South Australia. *Australian Journal of Earth Sciences* 1–7, doi: [10.1080/08120099.2018.1479306](https://doi.org/10.1080/08120099.2018.1479306)
- Eisenack A** (1965) Die Mikrofauna der Ostseekalke. 1. Chitinozoen, Hystrichosphären. *Neues Jahrbuch fuer Geologie und Palaeontologie, Abhandlungen* **123**, 149–59.
- Evans SD, Gehling JD and Droser ML** (2019) Slime travelers: early evidence of animal mobility and feeding in an organic mat world. *Geobiology* **17**, 490–509.
- Evitt WR** (1963) A discussion and proposals concerning fossil dinoflagellates, hystrichospheres, and acritarchs, I. *Proceedings of the National Academy of Sciences* **49**, 158–64.
- Gehling JG** (1999) Microbial mats in terminal Proterozoic siliciclastics; Ediacaran death masks. *Palaios* **14**, 40–57.
- Gehling JG and Droser ML** (2009) Textured organic surfaces associated with the Ediacara biota in South Australia. *Earth-Science Reviews*, **96**, 196–206.
- Gingras M, Hagadorn JW, Seilacher A, Lalonde SV, Pecoits E, Petrash D and Konhauser KO** (2011) Possible evolution of mobile animals in association with microbial mats. *Nature Geoscience* **4**, 372–5.
- Grant SWF** (1990) Shell structure and distribution of *Cloudina*, a potential index fossil for the terminal Proterozoic. *American Journal of Science* **290**, 261–94.
- Grazhdankin D and Gerdes G** (2007) Ediacaran microbial colonies. *Lethaia* **40**, 201–10.
- Grazhdankin DV, Marusin VV, Meert J, Krupenin MT and Maslov AV** (2011) Kotlin regional stage in the South Urals. *Doklady Earth Sciences* **440**, 1222–6.
- Grotzinger J, Adams EW and Schroder S** (2005) Microbial–metazoan reefs of the terminal Proterozoic Nama Group (c. 550–543 Ma), Namibia. *Geological Magazine* **142**, 499–517.
- Guilbaud R, Slater BJ, Poulton SW, Harvey THP, Brocks JJ, Nettersheim BJ and Butterfield NJ** (2018) Oxygen minimum zones in the early Cambrian ocean. *Geochemical Perspectives Letters* **6**, 33–8.
- Guiry MD and Guiry GM** (2008) *Nostoc. AlgaeBase*. World-wide electronic publication, National University of Ireland, Galway.
- Hermann, TN** (1974) Findings of mass accumulations of trichomes in the Riphean. In *Microfossils of Proterozoic and Early Paleozoic of the USSR* (ed. BV Timofeev), pp. 6–10. Leningrad: Nauka.
- Herringshaw LG, Callow RH and McIlroy D** (2017) Engineering the Cambrian explosion: the earliest bioturbators as ecosystem engineers. In *Earth System Evolution and Early Life: A Celebration of the Work of Martin Brasier* (eds AT Brasier, D McIlroy and N McLoughlin), pp. 369–82. Geological Society of London, Special Publication no. 448.
- Hofmann HJ and Jackson GD** (1994) *Shale-Facies Microfossils from the Proterozoic Bylot Supergroup, Baffin Island, Canada*. Washington, DC: The Paleontological Society, Memoir 37.
- Horodyski RJ** (1977) *Lyngbya* mats at Laguna Mormona, Baja California, Mexico; comparison with Proterozoic stromatolites. *Journal of Sedimentary Research* **47**, 1305–20.
- Hyypää J and Pekkala Y** (1987) *Tutkimustyö selostus Taivalkosken kunnassa valtausalueilla Saarijärvi 1-3 (kaiv.rek.nro 3156/1-3) suoritetuista savikivitutkimuksista*. Report M 06/3533/-87/1/89. Espoo: Geological Survey of Finland.
- Ivantsov AY, Nagovitsyn A and Zakrevskaya M** (2019b) Traces of locomotion of Ediacaran macroorganisms. *Geosciences* **9**, 1–11.
- Ivantsov AY, Zakrevskaya MA and Nagovitsyn AL** (2019a) Morphology of integuments of the Precambrian animals, Proarticulata. *Invertebrate Zoology* **16**, 19–26.
- Jankauskas TV** (1979) Srednerifeyski microbiota Yuzhnogo Urala i Bashkirskogo Priural’ya [Middle Riphean microbiota of the southern Urals and the Ural region in Bashkiria]. *Akademiï Nauk SSSR, Doklady* **248**, 190–3 (in Russian).
- Jankauskas TV, Mikhailova NS and Hermann TN** (1989) *Mikrofossilii Dokembriya SSSR [Precambrian Microfossils of the USSR]*. Leningrad: Nauka, 190 pp. (in Russian).
- Jannasch HW, Nelson DC and Wirsén CO** (1989) Massive natural occurrence of unusually large bacteria (*Beggiatoa* sp.) at a hydrothermal deep-sea vent site. *Nature* **342**, 834–6.
- Javaux EJ and Knoll AH** (2017) Micropaleontology of the lower Mesoproterozoic Roper Group, Australia, and implications for early eukaryotic evolution. *Journal of Paleontology* **91**, 199–229.

- Jensen S (2003) The Proterozoic and earliest Cambrian trace fossil record: patterns, problems and perspectives. *Integrative and Comparative Biology* **43**, 219–28.
- Jensen S, Droser ML and Gehling JG (2005) Trace fossil preservation and the early evolution of animals. *Palaeogeography, Palaeoclimatology, Palaeoecology* **220**, 19–29.
- Jensen S, Droser ML and Gehling JG (2006) A critical look at the Ediacaran trace fossil record. In *Neoproterozoic Geobiology and Paleobiology* (eds S Xiao and AJ Kaufman), pp. 115–57. Dordrecht: Springer.
- Jensen S, Saylor BZ, Gehling JG and Germs GJB (2000) Complex trace fossils from the terminal Proterozoic of Namibia. *Geology* **28**, 143–6.
- Kesidis G, Slater BJ, Jensen S and Budd GE (2019) Caught in the act: priapulid burrowers in Early Cambrian substrates. *Proceedings of the Royal Society B* **20182505**. doi: [10.1098/rspb.2018.2505](https://doi.org/10.1098/rspb.2018.2505).
- Klein R, Salminen J and Mertanen S (2015) Baltica during the Ediacaran and Cambrian: a paleomagnetic study of Hailuoto sediments in Finland. *Precambrian Research* **267**, 94–105.
- Knoll AH, Javaux EJ, Hewitt D and Cohen P (2006) Eukaryotic organisms in Proterozoic oceans. *Philosophical Transactions of the Royal Society B: Biological Sciences* **361**, 1023–38.
- Knoll AH, Swett K and Mark J (1991) Paleobiology of a Neoproterozoic tidal flat/lagoonal complex: the Draken Conglomerate Formation, Spitsbergen. *Journal of Paleontology* **65**, 531–70.
- Knoll AH, Wörndle S and Kah LC (2013) Covariance of microfossil assemblages and microbialite textures across an upper Mesoproterozoic carbonate platform. *Palaios* **28**, 453–70.
- Kohonen J and Rämö OT (2005) Sedimentary rocks, diabases, and late cratonic evolution. In *Precambrian Geology of Finland: Key to the Evolution of the Fennoscandian Shield* (eds M Lehtinen, PA Nurmi and OT Rämö), pp. 563–604. Amsterdam: Elsevier.
- Kouchinsky A, Bengtson S, Runnegar B, Skovsted C, Steiner M and Vendrasco M (2012) Chronology of early Cambrian biomineralization. *Geological Magazine* **149**, 221–51.
- Kumar S (2001) Mesoproterozoic megafossil Chuar–Tawua association may represent parts of a multicellular plant, Vindhyan Supergroup, Central India. *Precambrian Research* **106**, 187–211.
- Laing BA, Mángano MG, Buatois LA, Narbonne GM and Gougeon RC (2019) A protracted Ediacaran–Cambrian transition: an ichnologic ecospace analysis of the Fortunian in Newfoundland, Canada. *Geological Magazine* **156**, 1–8.
- Lamont HC (1969) Sacrificial cell death and trichome breakage in an oscillatoriacean blue-green alga: the role of murein. *Archiv für Mikrobiologie* **69**, 237–59.
- Leonov MV and Ragozina AL (2007) Upper Vendian assemblages of carbonaceous micro- and macrofossils in the White Sea Region: systematic and biostratigraphic aspects. In *The Rise and Fall of the Ediacaran Biota* (eds P Vickers-Rich and P Komarower), pp. 269–75. Geological Society of London, Special Publication no. 286.
- Li G, Pang K, Chen L, Zhou G, Han C, Yang L, Wang W, Yang F and Yin L (2019). Organic-walled microfossils from the Tonian Tongjiashuang Formation of the Tumen Group in western Shandong, North China Craton and their biostratigraphic significance. *Gondwana Research* **76**, 260–89.
- Lidmar-Bergström K (1993) Denudation surfaces and tectonics in the southernmost part of the Baltic Shield. *Precambrian Research* **64**, 337–45.
- Lidmar-Bergström K (1995) Relief and saprolites through time on the Baltic Shield. *Geomorphology* **12**, 45–61.
- Liu AG, Matthews JJ, Menon LR, McIlroy D and Brasier MD (2014) *Haootia quadriformis* n. gen., n. sp., interpreted as a muscular cnidarian impression from the Late Ediacaran period (approx. 560 Ma). *Proceedings of the Royal Society B: Biological Sciences* **281**, 20141202.
- Liu Y, Li Y, Shao T, Zhang H, Wang Q and Qiao J (2014) *Quadrasyrgites* from the lower Cambrian of South China: growth pattern, post-embryonic development, and affinity. *Chinese Science Bulletin* **59**, 4086–95.
- Liu Y, Shao T, Zhang H, Wang Q, Zhang Y, Chen C, Liang Y and Xue J (2017) A new scyphozoan from the Cambrian Fortunian Stage of South China. *Palaentology* **60**, 511–8.
- Loron C and Moczyłowska M (2018) Tonian (Neoproterozoic) eukaryotic and prokaryotic organic-walled microfossils from the upper Visingsö Group, Sweden. *Palynology* **42**, 220–54.
- Loron CC, Rainbird RH, Turner EC, Greenman JW and Javaux EJ (2019) Organic-walled microfossils from the late Mesoproterozoic to early Neoproterozoic lower Shaler Supergroup (Arctic Canada): diversity and biostratigraphic significance. *Precambrian Research* **321**, 349–74.
- Luukas J, Kousa J, Nironen M and Vuollo J (2017) Major stratigraphic units in the bedrock of Finland, and an approach to tectonostratigraphic division. *Geological Survey of Finland Special Papers* **60**, 9–40.
- Marlétaz F, Peijnenburg KT, Goto T, Satoh N and Rokhsar DS (2019) A new spiralian phylogeny places the enigmatic arrow worms among gnathiferans. *Current Biology* **29**, 312–8.
- Martí Mus M (2014) Interpreting ‘shelly’ fossils preserved as organic films: the case of hyolithids. *Lethaia* **47**, 397–404.
- Martin MW, Grazhdankin DV, Bowring SA, Evans DAD, Fedonkin MA and Kirschvink JL (2000) Age of Neoproterozoic bilaterian body and trace fossils, White Sea, Russia: implications for metazoan evolution. *Science* **288**, 841–5.
- McIlroy D and Logan GA (1999) The impact of bioturbation on infaunal ecology and evolution during the Proterozoic–Cambrian transition. *Palaios* **14**, 58–72.
- Meidla T (2017) Ediacaran and Cambrian stratigraphy in Estonia: an updated review. *Estonian Journal of Earth Sciences* **66**, 152–60.
- Mendoza-Becerril MA, Maronna MM, Pacheco ML, Simões MG, Leme JM, Miranda LS, Morandini AC and Marques AC (2016) An evolutionary comparative analysis of the medusozoan (Cnidaria) exoskeleton. *Zoological Journal of the Linnean Society* **178**, 206–25.
- Mens K and Pirrus E (1997) Cambrian. In *Geology and Mineral Resources of Estonia* (eds A Raukas and A Teedumae), pp. 39–51. Tallinn: Estonian Academy of Sciences.
- Meyer M, Xiao S, Gill BC, Schiffbauer JD, Chen Z, Zhou C and Yuan X (2014) Interactions between Ediacaran animals and microbial mats: insights from *Lamonte trevallisi*, a new trace fossil from the Dengying Formation of South China. *Palaeogeography, Palaeoclimatology, Palaeoecology* **396**, 62–74.
- Moczyłowska M (2005) Taxonomic review of some Ediacaran acritarchs from the Siberian Platform. *Precambrian Research* **136**, 283–307.
- Moczyłowska M (2008) The Ediacaran microbiota and the survival of Snowball Earth conditions. *Precambrian Research* **167**, 1–15.
- Moczyłowska M, Pease V, Willman S, Wickström L and Agić H (2017) A Tonian age for the Visingsö Group in Sweden constrained by detrital zircon dating and biochronology: implications for evolutionary events. *Geological Magazine* **155**, 1175–89.
- Mollenhauer D, Bengtsson R and Lindström EA (1999) Macroscopic cyanobacteria of the genus *Nostoc*: a neglected and endangered constituent of European inland aquatic biodiversity. *European Journal of Phycology* **34**, 349–60.
- Nagarkar S (2002) Morphology and ecology of new records of cyanobacteria belonging to the genus *Oscillatoria* from Hong Kong rocky shores. *Botanica Marina* **45**, 274–83.
- Narbonne GM (2005) The Ediacara biota: Neoproterozoic origin of animals and their ecosystems. *Annual Review of Earth and Planetary Sciences* **33**, 421–42.
- Nielsen AT and Schovsbo NH (2011) The Lower Cambrian of Scandinavia: depositional environment, sequence stratigraphy and palaeogeography. *Earth-Science Reviews* **107**, 207–310.
- Öhman T and Preeden U (2013) Shock metamorphic features in quartz grains from the Saarijärvi and Söderfjärden impact structures, Finland. *Meteoritics and Planetary Science* **48**, 955–75.
- Paulamäki S and Kuivamäki A (2006) Depositional history and tectonic regimes within and in the margins of the Fennoscandian Shield during the last 1300 million years. *Posiva Working Report 2006-43*, 128 pp.
- Penny AM, Wood R, Curtis A, Bowyer F, Tostevin R and Hoffman KH (2014) Ediacaran metazoan reefs from the Nama Group, Namibia. *Science* **344**, 1504–6.



- Pjatiletov VG** (1988) Mikrofitofossiliit Pozdnego Dokembriia Uchuro-Maiskogo Raiona (late Precambrian microphytofossils from the Uchur-Maya region). In *Pozdniei Dokembrii I Rannii Paleozoi Sibiri Rifei I Vend* (eds VV Khomentovsky and VY Shenfil), pp. 47–104. Novosibirsk: Institut Geologii I Geofiziki, Akademiia Nauk SSSR, Sibirskoe Otdelenie.
- Porter SM and Riedman LA** (2016) Systematics of organic-walled microfossils from the ca. 780–740 Ma Chuar Group, Grand Canyon, Arizona. *Journal of Paleontology* **90**, 815–53.
- Puura V, Amantov A, Tikhomirov S and Laitakari I** (1996) Latest events affecting the Precambrian basement, Gulf of Finland and surrounding areas. *Geological Survey of Finland, Special Paper* **21**, 115–25.
- Rani VU, Perumal UE and Palanivel S** (2016) Morphology and taxonomy of *Oscillatoria princeps* Vaucher ex gomont (oscillatoriaceae). *Indian Journal of Education and Information Management* **5**, 1–5.
- Riedman LA and Porter S** (2016) Organic-walled microfossils of the mid-Neoproterozoic Alinya Formation, Officer Basin, Australia. *Journal of Paleontology* **90**, 854–87.
- Riedman LA, Porter SM, Halverson GP, Hurtgen MT and Junium CK** (2014) Organic-walled microfossil assemblages from glacial and interglacial Neoproterozoic units of Australia and Svalbard. *Geology* **42**, 1011–14.
- Rieger GE and Rieger RM** (1977) Comparative fine structure study of the Gastrotrich cuticle and aspects of cuticle evolution within the Aschelminthes 1. *Journal of Zoological Systematics and Evolutionary Research* **15**, 81–124.
- Samuelsson J and Butterfield NJ** (2001) Neoproterozoic fossils from the Franklin Mountains, northwestern Canada: stratigraphic and palaeobiological implications. *Precambrian Research* **107**, 235–51.
- Schiffbauer JD, Huntley JW, O'Neil GR, Darroch SA, Laflamme M and Cai Y** (2016) The latest Ediacaran Wormworld fauna: setting the ecological stage for the Cambrian Explosion. *GSA Today* **26**, 4–11.
- Schopf JW** (1968) Microflora of the Bitter Springs formation, late Precambrian, central Australia. *Journal of Paleontology* **42**, 651–88.
- Seilacher A** (1999) Biomat-related lifestyles in the Precambrian. *Palaiois* **14**, 86–93.
- Seilacher A, Buatois LA and Mángano MG** (2005) Trace fossils in the Ediacaran–Cambrian transition: behavioral diversification, ecological turnover and environmental shift. *Palaeogeography, Palaeoclimatology, Palaeoecology* **227**, 323–56.
- Sergeev VN, Knoll AH and Vorob'eva NG** (2011) Ediacaran microfossils from the Ura Formation, Baikal-Patom Uplift, Siberia: taxonomy and biostratigraphic significance. *Journal of Paleontology* **85**, 987–1011.
- Sergeev VN, Knoll AH, Vorob'eva NG and Sergeeva ND** (2016) Microfossils from the lower Mesoproterozoic Kaltasy Formation, East European Platform. *Precambrian Research* **278**, 87–107.
- Sharma M and Shukla Y** (2012) Occurrence of helically coiled microfossil *Obruchevella* in the Owk Shale of the Kurnool Group and its significance. *Journal of Earth System Science* **121**, 755–68.
- Shepeleva ED** (1973) Raschlenenie Venda Russkoy Platformy no Akritarham. Mikrofitofossiliit drevnejshikh otlozhenij, 13–15.
- Shukovsky ES and Halfen LN** (1976) Cellular differentiation of terminal regions of trichomes of *oscillatoria princeps* (cyanophyceae) 1. *Journal of Phycology* **12**, 336–42.
- Sili C, Torzillo G and Vonshak A** (2012) Arthrospira (Spirulina). In *Ecology of Cyanobacteria II* (ed. BA Whitton), pp. 677–705. Dordrecht: Springer.
- Slater BJ** (2018) Opening a new window onto the Cambrian Explosion of animal life. *Palaentological Association Newsletter* **98**, 85–7.
- Slater BJ and Budd GE** (2019) Comment on: Tang et al. [2019]: A problematic animal fossil from the early Cambrian Hetang Formation, South China. *Journal of Paleontology* **93**, 1276–8.
- Slater BJ, Harvey THP, Bekker A and Butterfield NJ** (2020) *Cochleatina*: an enigmatic Ediacaran–Cambrian survivor among small carbonaceous fossils (SCFs). *Palaentology* **63**, 733–52.
- Slater BJ, Harvey THP and Butterfield NJ** (2018a) Small carbonaceous fossils (SCFs) from the Terreneuvian (lower Cambrian) of Baltica. *Palaentology* **61**, 417–39.
- Slater BJ, Harvey THP, Guilbaud R and Butterfield NJ** (2017) A cryptic record of Burgess Shale-type diversity from the early Cambrian of Baltica. *Palaentology* **60**, 117–40.
- Slater BJ and Willman S** (2019) Early Cambrian small carbonaceous fossils (SCFs) from an impact crater in western Finland. *Lethaia* **52**, 570–82.
- Slater BJ, Willman S, Budd GE and Peel JS** (2018b) Widespread preservation of small carbonaceous fossils (SCFs) in the early Cambrian of North Greenland. *Geology* **46**, 107–10.
- Smith MR, Harvey THP and Butterfield NJ** (2015) The macro- and microfossil record of the Cambrian priapulid *Ottoia*. *Palaentology* **58**, 705–21.
- Solismaa LM** (2008) *Hailuodon ja Muhoksen muodostumien sedimentologiasta ja strigrafiasta* [On the sedimentology and stratigraphy of the Hailuoto and Muhos Formations]. Master's thesis. University of Turku, Finland, 106 pp. (in Finnish).
- Speziale BJ and Dyck LA** (1992) Lyngbya infestations: comparative taxonomy of *Lyngbya wollei* comb. nov. (cyanobacteria) 1. *Journal of Phycology* **28**, 693–706.
- Stanley SM** (1973) An ecological theory for the sudden origin of multicellular life in the late Precambrian. *Proceedings of the National Academy of Sciences* **70**, 1486–9.
- Steiner M and Reitner J** (2001) Evidence of organic structures in Ediacara-type fossils and associated microbial mats. *Geology* **29**, 1119–22.
- Tang Q, Pang K, Yuan X and Xiao S** (2017) Electron microscopy reveals evidence for simple multicellularity in the Proterozoic fossil *Chuaria*. *Geology* **45**, 75–8.
- Tarhan LG, Droser ML, Gehling JG and Dzaugis MP** (2017) Microbial mat sandwiches and other anactualistic sedimentary features of the Ediacara Member (Rawnsley Quartzite, South Australia): implications for interpretation of the Ediacaran sedimentary record. *Palaiois* **32**, 181–94.
- Timofeev BV** (1959) The ancient flora of the Baltic region and its stratigraphic significance. *Trudy VNIIGRI* **129**, 1–320.
- Timofeev BV** (1966) *Mikropaleofitologicheskoe Issledovanie Drevnikh Svit*. [Micropaleontological Investigations of Ancient Formations]. Moscow: Akademiya Nauk SSSR, Isdatelskvo Nauka, 147 pp.
- Timofeev BV and Hermann TN** (1979) Precambrian microbiota of the Lakhanda Formation. In *Palaentology of the Precambrian and Early Cambrian*, pp. 137–47. Leningrad: Nauka (in Russian).
- Timofeev BV, Hermann TN and Mikhailova NS** (1976) *Microphytofossils from the Precambrian, Cambrian and Ordovician*. Leningrad: Nauka, 106 pp.
- Tynni R and Donner J** (1980) A microfossil and sedimentation study of the Late Precambrian formation of Hailuoto, Finland. *Geological Survey of Finland Bulletin* **311**, 1–27.
- Tynni R and Donner J** (1982) Validation of some late Precambrian microfossil species from the Hailuoto Formation, Finland. *Journal of Paleontology* **56**, 754.
- Tynni R and Siivola J** (1966) On the Precambrian microfossil flora in the siltstone of Muhos, Finland. *Bulletin de la Commission Géologique de Finlande* **222**, 127–33.
- Tynni R and Uutela A** (1984) Microfossils from the Precambrian Muhos formation in western Finland. *Geological Survey of Finland Bulletin* **300**, 1–60.
- Tynni R and Uutela A** (1985) Myöhäisprekambrinen ajoitus Taivalkosken savikivelle mikrofitofossiliien perusteella. Summary: Late Precambrian shale formation of Taivalkoski in northern Finland. *Geologi* **37**, 61–5.
- Veltheim V** (1969) On the pre-Quaternary geology of the Bothnian Bay area in the Baltic Sea. *Bulletin de la Commission Géologique de Finlande* **239**, 1–56.
- Vidal G and Moczydlowska M** (1992) Patterns of phytoplankton radiation across the Precambrian–Cambrian boundary. *Journal of the Geological Society* **149**, 647–54.
- Wallet E, Slater BJ, Willman S and Peel JS** (2021) Small carbonaceous fossils (SCFs) from North Greenland: new light on metazoan diversity in early Cambrian shelf environments. *Papers in Palaentology* **7**, 1403–1433.
- Wang Y, Wang Y and Du W** (2017) A rare disc-like holdfast of the Ediacaran macroalga from South China. *Journal of Paleontology* **91**, 1091–1101.
- Warren LV, Pacheco MLAF, Fairchild TR, Simões MG, Riccomini C, Boggiani PC and Cáceres AA** (2012) The dawn of animal skeletogenesis:

- ultrastructural analysis of the Ediacaran metazoan *Corumbella weneri*. *Geology* **40**, 691–4.
- Williams LA and Reimers C** (1983) Role of bacterial mats in oxygen-deficient marine basins and coastal upwelling regimes: Preliminary report. *Geology* **11**, 267–9.
- Willman S, Moczyłowska M and Grey K** (2006) Neoproterozoic (Ediacaran) diversification of acritarchs: a new record from the Murnaroo 1 drillcore, eastern Officer Basin, Australia. *Review of Palaeobotany and Palynology* **139**, 17–39.
- Willman S, Peel JS, Ineson JR, Schovsbo NH, Rugen EJ and Frei R** (2020) Ediacaran Doushantuo-Type biota discovered in Laurentia. *Communications Biology* **3**, 1–10. doi: [10.1038/s42003-020-01381-7](https://doi.org/10.1038/s42003-020-01381-7)
- Yun Z** (1981) Proterozoic stromatolite microfloras of the Gaoyuzhuang Formation (Early Sinian: Riphean), Hebei, China. *Journal of Paleontology* **55**, 485–506.